

MINERALOGY AND GEOCHEMISTRY OF THE HEMATITE MUSCOVITE SCHISTS OF MALATYA, TURKEY: COULD IT BE THE FIRST KNOWN BANDED IRON FORMATION (BIF) IN THE TAURIDS AND ANATOLIA?

Ahmet SAGIROGLU^{1*}, Hatice KARA¹ & Sevcan KÜRÜM¹

¹Geology Department, Firat University, Elazig, Turkey, *sagioglu@firat.edu.tr

Abstract: The Hematite Mica Schist (HMS) of Malatya outcrops as a thrust slice between the Permian Malatya Metamorphics and the Eocene Maden Complex and probably as a portion of the Neoproterozoic-Paleozoic Pütürge Massif. The HMS is composed of laminae of quartz, mica-disthene (kyanite)-diopside –garnet and specular hematite. The Fe₂O₃ contents (>20 %) of the HMS and the Al₂O₃ contents (average 22 %) are different from those of Proterozoic BIFs. The TiO₂, K₂O, MgO, CaO and Na₂O contents are much higher than BIFs and average crust values, indicating detrital origin. Trace element and V, Sr, Y, Zr, Nb and Ba contents are higher than in BIFs. Total REE contents of the HMS are also much higher than those of BIFs of Proterozoic age, and the LREE concentrations are significantly higher than HREE concentrations, both of these indicators can be taken as evidence of detrital origin. Malatya HMS show strong positive Eu anomalies (Eu/Eu*=0.99-1.03) probably originating from a detrital feldspar contribution. The Ce anomalies (Ce/Ce*= 0.003-0.06) of HMS are low positive, indicating a low oxidation state. Data obtained from the studies suggest that the HMS was formed in glaciomarine settings (Raptian Type) with a low oxidation state, high detrital contribution, low or no hydrothermal contribution. Despite some contradictions in the geochemistry; the HMS show similarities to Raptian Type Neoproterozoic BIFs/IFs of Egypt and Saudi Arabia. As the cores of the Anatolian massifs are accepted northern margins of African/Arabian plate, the HMS may be related to the African/Arabian plate and their Raptian Type neoproterozoic iron formations. Banded Iron Formations (BIFs) are not known in Anatolian geologic environment, and the HMS of Malatya constitute evidence resembling Neoproterozoic BIF .

Key words: Hematite mica schist, banded iron formations, Neoproterozoic, Taurids-Turkey, Pütürge Massif

1. INTRODUCTION

This research investigates the mineralogy and geochemistry of hematite-mica schist of Malatya, Eastern Taurid, and compares the schist with Banded Iron Formations. The existence potential of Banded Iron Formations in Eastern Taurid Region is discussed. The hematite-muscovite schist (HMS) outcrops in a narrow area in front of a thrust zone which thrust Permian Malatya Metamorphics over the Eocene Maden Complex. The HMS does not exhibit features of Malatya Metamorphics instead it bears clear evidences of high grade metamorphic conditions. The only high grade metamorphic unit in the vicinity is the Pütürge Massif and the HMS probably is a portion of this unit.

Prior to the 1990s the “massif”s of Turkey

were believed to be of Paleozoic age (Yılmaz, 1991; Yazgan, 1984; Özgül, 1976). However, recent studies (Candan et al., 2011; Oberhansli et al., 2010; Bozkurt et al., 2008; Bozkurt et al., 2006; Anders et al., 2006; Ustaömer et al., 2005; Gessner et al., 2004; Oberhansli et al., 1997; Bozkurt et al., 1993) on the geology of Turkey show that the so called “massif”s are not Paleozoic as a whole and that they have Neoproterozoic cores. Therefore, it is reasonable to assume that they may include economic deposits formed in Precambrian geological environments, i.e. Banded Iron Formations.

Banded Iron Formations (BIFs) occur in the Precambrian sedimentary (Superior Type) and volcano sedimentary (Algoma Type) successions. Recent studies (Basta et al., 2011; Bekker et al.,

2010; Gutzmer et al., 2008) describes glacial association BIFs of Raptian Type. Because of their vast ore reserves, they have economic value as prime resources of iron ore. Most of the BIFs show fine laminations and micro bandings of chert and iron oxides (carbonates). The BIFs deposition begin at 3.8 Ga, the formations reach a maximum at about 2.5 Ga, disappear at 1.8 Ga and briefly reappear between 0.8- 0.6 Ga. (Basta et al., 2011; Ilyin, 2009; Klein, 2005; Klein & Laderia, 2004). Major BIF depositions formed as a result of the first great rise in atmospheric oxygen, the Great Oxidation Event (GEO) that is thought to have occurred between 2.4 and 2.2 Ga ago and after billions of years of oxygen deficient or low oxygen bearing atmosphere (Bekker & Kaufman, 2007; Kump & Seyfried, 2005; Morris, 1993; Holland, 1984).

After a hiatus of over a billion year, BIFs reappeared in Neoproterozoic successions (Bekker et al., 2010; Pecoits et al., 2008; Scott et al., 2008; Pelletier et al., 2006). Freitas et al., (2011) called Neoproterozoic Iron Formations (NIF) and studies on the subject (Freitas et al., 2011; Eyles & Januszczak, 2004; Klein & Beukes, 1993) concluded that NIFs occurred as a result of oxygenation of the hydrosphere after the melting of ice cover on the oceans. According to Basta et al., (2011) Neoproterozoic Algoma type (of volcanic association) NIFs occur in African and Arabian shield, whereas Raptian types (of glacial association) are present on all over the continents.

2. GEOLOGICAL SETTING

The Malatya HMS studied here is situated about 15 kms southeast of Malatya township, by the Malatya- Sincik highway and exist as a small tectonic slice in front of the thrust zone that pushed the Carboniferous-Triassic (Bozkaya et al., 2006, 2007; Özgül, 1976) Malatya Metamorphics over the Eocene Maden Complex (Fig. 1). The Malatya Metamorphics form one of the three structural units (the other two are Bitlis –Pütürge and Keban Metamorphics) of the Southeast Anatolian Metamorphic Complexes. The Malatya Metamorphics are dominated by metacarbonates, and metapelites (shale, calc schist) are subordinate. These two groups of lithologies were metamorphosed under sub-greenschist facies conditions (Bozkaya et al., 2007).

Precambrian-Permian Pütürge Metamorphics are overlain by the Maden Complex and are composed of high grade metamorphic rocks. The Eocene Maden Complex is composed of volcanic, volcano sedimentary and sedimentary units and

overlies the Pütürge Massif with a basal conglomerate.

The HMS was emplaced between the Maden Complex and the metacarbonates of the Malatya Metamorphics and only a small portion of it is exposed by newly opened road cuts. It covers an area of 200-300 sq meters. The rock is fragmented, probably due to thrust movement, and the original texture is observable only in blocks. Laminated texture is clearly visible to the naked eye (Fig. 2a).

3. PETROGRAPHY

The hematite mica schist is composed of alternating laminae of chert, hematite and mica-kyanite (Fig. 2b). The chert bands are thicker than the other two and this feature is reflected in the geochemistry of the schist with SiO₂ contents in excess of 40 %. The iron rich bands are composed of specular hematite (specularite) laths what are elongated along schistosity and show microfoldings (Fig. 2c). The mica is muscovite and has a pale green color under the microscope. The mica bands also include kyanite, clinopyroxene (diopside), garnet (almandine), feldspars and titanite. Kyanite is prismatic and the prisms are elongated parallel to the banding/schistosity. Muscovite bands show micro-folding and schistosity. Zircon is present in all bands and occurs as short prismatic crystals.

Mineral assemblage of the hematite mica schist represents amphibolite facies metamorphism of clayey sediments.

4. GEOCHEMISTRY

Since the hematite-schist exposures cover only a few hundreds of square meters, four samples representing the exposure were chosen and analyzed at ACME Labs Canada using ICP-MS techniques. The same samples were also analyzed using XRF techniques at Analytical Labs, Mersin University, Turkey.

The major, trace and REE data of the Hematite-Schist are given in Tables 1, 2 and 3, respectively. The SiO₂ contents are paramount as is to be expected from the petrography of the HMS. The Fe₂O₃ contents are at the lower limits of BIF and vary between 17 and 23 % and the Al₂O₃ contents are remarkably high probably due to the presence of large amounts of aluminous-silicates in mica bands. The TiO₂ contents are also high and vary about 4% as expected from the common presence of titanite. The HMS contains large amounts of REE and exhibits different features what are discussed below, than BIFs. V, Sr, Zr, Nb and Ba

contents of the HMS are much higher than those of similar iron formations in the literature.

5. DISCUSSIONS

Apart from a vague description by Küpeli et al., (2007) as “Precambrian sedimentary Fe-sulfides and oxides observed at the basement of the Attepe Formation”, any formation with features similar to BIF has not been documented in Turkey before. In fact, until the late 1990s Precambrian formations were not known in Turkey and the oldest geological units, massifs, were estimated as Paleozoic age and BIFs and similar Precambrian formations have not been sought in the massifs. Recent absolute age determinations (Menderes Massif 699-713 my,

Anders et al., 2006; Istanbul Zone Magmatics 575-700 my, Sunal et al., 2008; Bolu Massif 565-576 my, Ustaömer et al., 2005) proved that the massifs have, at least, Proterozoic cores. The hematite schist studied here is probably a portion of the Proterozoic core of the Pütürge Massif of which exposed parts are composed of mica schist, amphibole schist, amphibolite, gneiss, augen gneiss and marble. Any formation resembling the HMS has not been documented in the exposed parts of the Pütürge Massif. The only unit with comparable features to the HMS is the mica gneiss which contains abundant kyanite and pyrophyllite, but no hematite, and covers large areas in south of Pütürge township. Pyrophyllite is formed in the shear zones of the mica schist and probably as product of retrograde metamorphism.

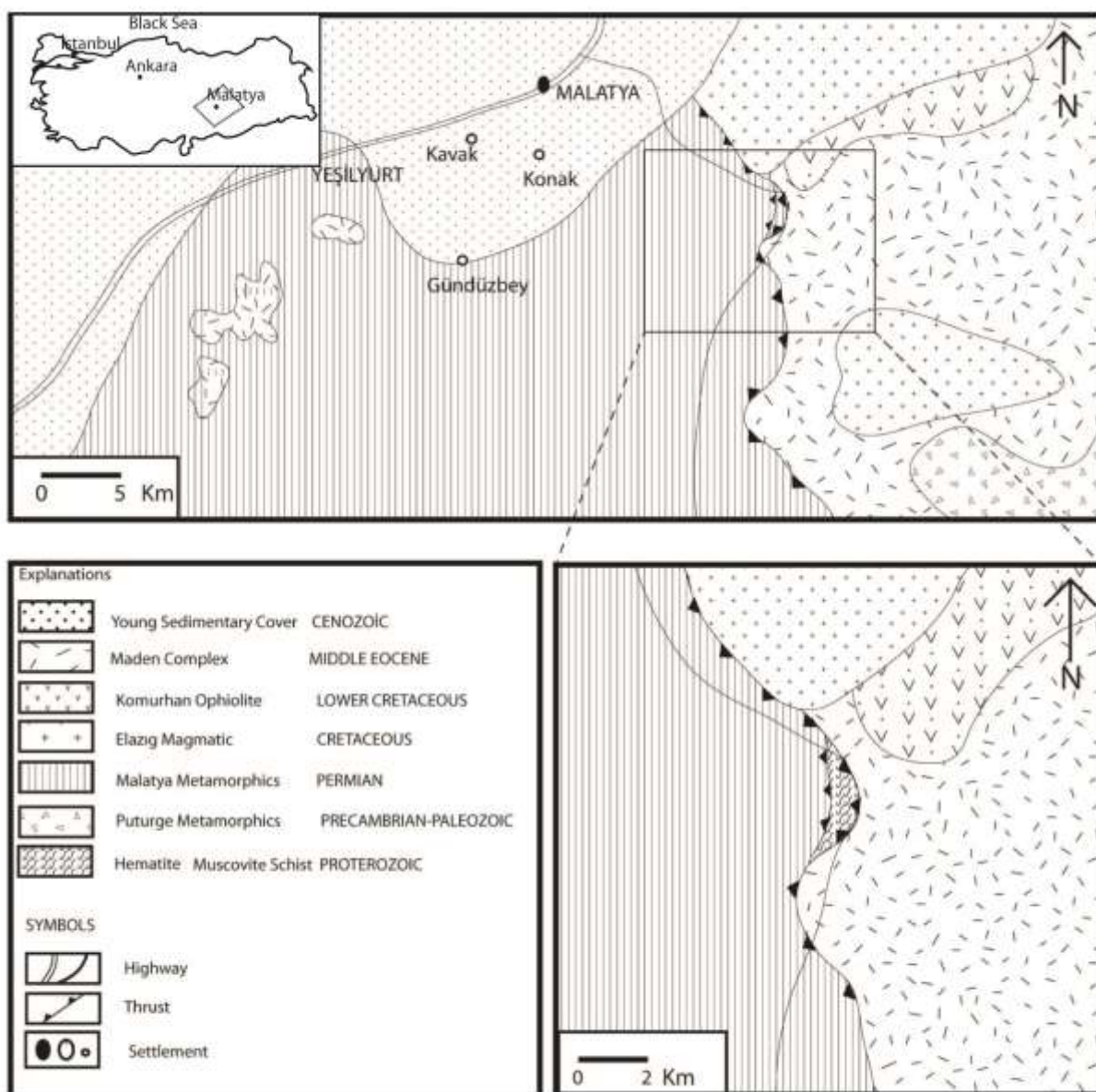


Figure 1. Simplified geological map of the hematite- muscovite-schist and surroundings (based on MTA 2002).

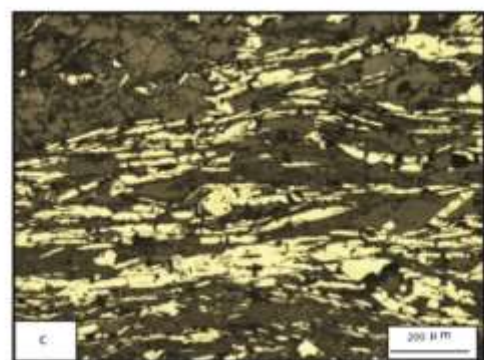


Figure 2. Photos of hematite-muscovite-schist. (a) Hand specimen of the HMS. Laminae of hematite (bright levels) and mica are visible with naked eye. (b) Transmitted light photomicrograph; light green colored minerals are mica, quartz levels are white and dark minerals are hematite. (c) Reflected light photomicrograph, bright crystals are hematite laths and prisms. Note the micro foldings.

Major element contents of the HMS show differences in comparison with BIFs. Fe contents are very low, just above the lower limit of BIF's (Table 1).

SiO₂ contents are within the range of those of BIF. Al₂O₃ contents are significantly higher than Al₂O₃ contents of BIF but similar to those of schists underlying and/or overlying Eastern India BIF zones (Roy & Venkatesh 2009). Large alumina contents may be attributed to the detrital material input to the sedimentary basin where the HMS was deposited. Therefore, any hydrothermal contribution to the HMS deposition was unlikely. The MgO, CaO, Na₂O, K₂O and especially TiO₂ contents are all

higher than those of BIFs and support a sedimentary origin. High contents of Na₂O and K₂O indicate that pyroclastic debris was present during the sedimentation of the HMS. Plots of crust-normalized major elements (Fig. 3) show strong positive anomalies, specifically for Fe, Al and Ti. Trace element contents (Table 2) are generally higher and V, Sr, Y, Zr, Nb and Ba contents significantly higher than trace element contents of BIFs (Fig. 4). From Table 2 and Figure 4, it can be seen that the total amount of trace elements of the HMS is many times higher than that of BIFs. (Co+Cu+Ni)/ΣREE plots can be used to differentiate hydrothermal from hydrogenous deposits (Bhattacharya, et al., 2007).

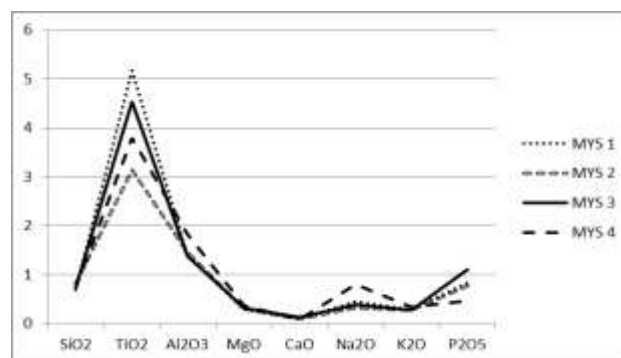


Figure 3. Plots of average crust normalized major elements of Malatya HMS. SiO₂, TiO₂ and Al₂O₃ contents much higher than those of crustal average, alkaline elements are lower.

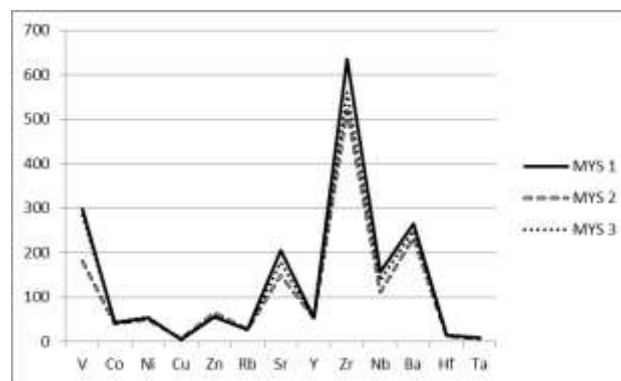


Figure 4. Plots of trace elements of Malatya hematite-muscovite-schist. Vertical axis show absolute contents as ppm.

Figure 5a indicates that ΣREE contents are very similar to those of Hydrogenous Deep-Sea Deposits. However, Co+Ni+Co contents are not as high and are similar to Hydrothermal Deep Sea Deposits. The SiO₂-Al₂O₃ plots, which may also be used to discriminate between sources, fall in the area close to deep sea sediments area (Fig. 5b).

The total REE contents of the HMS are tens of times higher than those of BIFs of Proterozoic age (Table 3, Fig. 6).

Table 1. Major elements contents of the HMS compared with major BIFs of the world. First 4 data are of this study. Note the much higher Al₂O₃, TiO₂ and lower Fe₂O₃ values.

	MYS1	MYS2	MYS3	MYS4	Kuruman-Penge ¹	Urucum ²	Brockman ³	Sundur SB ⁴	Carajas ⁵	Superior type-BIF ⁶
SiO ₂	41.89	48.76	43.95	44.33	51.68	34.30	45.76	40.60	41.50	47.30
TiO ₂	5.49	3.32	4.81	4.03	0.02	0.09	0.01	0.02	0.02	0.04
Al ₂ O ₃	21.78	22.75	21.57	28.6	0.11	0.87	0.09	0.10	0.09	1.07
Fe ₂ O ₃	23.21	17.70	22.37	16.36	39.79	56.6	49.17	58.70	57.70	43.10
MgO	1.05	1.09	1.13	1.35	5.14	1.10	2.85	0.26	0.03	5.68
CaO	0.55	0.53	0.63	0.45	5.65	2.63	1.75	0.05	0.02	3.03
Na ₂ O	1.76	1.27	1.51	3.11	0.03	0.32	0.04	0.01	0.01	0.33
K ₂ O	0.93	0.89	0.89	1.11	0.03	0.02	0.02	0.02	0.01	0.27
P ₂ O ₃	0.25	0.23	0.33	0.14	0.09	0.29	0.22	0.04	0.02	0.10
LOI	2.70	3.20	2.50	N.A	N.A	N.A	N.A	0.04	0.04	N.A
Total	96.91	99.74	99.69	99.48	102.54	96.22	99.91	99.84	99.43	100.92

¹⁻³Klein & Beukes, 1992; ²Klein & Ladeira, 2004; ⁴This study; ⁵Figueiredo - Silva et al., 2008 and Klein & Ladeira, 2002; ⁶McClung, 2006; N.A: not analyzed.

Table 2. Trace elements contents of the HMS compared with BIFs from the world. Generally trace element contents are higher than trace element contents of known BIF deposits.

Ppm	QF Hematite Itabirite		QF Itabirite	QF Itabirite	Superio BIF	Algoma BIF	Nigeria BIF	Orrissa IndiaBIF	Trace Elements This Study		
	MYS1	MYS2	MYS3	MYS4	MYS1	MYS2	MYS3	MYS1	MYS2	MYS3	
V	39.0	20.6	22.6	-	30.0	97.0	44.0	30.0	299.0	180.0	284.0
Co	9.0	21.6	-	249.0	27.0	38.0	100.0	35.0	42.1	40.9	44.6
Ni	5.5	11.3	10.5	20.0	32.0	83.0	<10	15.0	54.3	50.1	54.8
Cu	2.9	3.9	<1.0	33.8	10.0	96.0	<10	10.0	5.3	7.0	4.8
Zn	4.4	2.0	-	42.3	2.0	33.0	26.0	-	55.0	65.0	57.0
Rb	0.6	0.5	<1.0	32.9	-	-	20.0	-	27.1	27.1	26.7
Sr	3.7	4.6	5.0	10.3	42.0	83.0	51.0	15.0	205.7	149.5	178.6
Y	8.2	5.0	3.9	4.8	41.0	54.0	22.0	-	53.0	53.6	52.3
Zr	7.0	3.0	12.0	2.5	60.0	84.0	60.0	10.0	635.1	519.7	559.9
Nb	1.4	1.3	0.8	6.4	-	-	5.0	-	156.9	111.2	137.2
Ba	10.8	13.3	15.4	55.4	180.0	170.0	293.0	70.0	265.0	234.0	250.0
Hf	0.3	0.3	<0.1	0.1	-	-	-	-	15.4	12.5	12.7
Ta	0.1	0.3	-	0.1	-	-	-	-	8.7	6.3	7.6
ΣTE	92.6	87.9	72.3	457.3	424.0	738.0	621.0	185.0	1822.6	1456.9	1678.3

The LREE concentrations of the HMS are significantly higher than HREE concentrations, and that may be attributed to detrital origin (Klein & Ladeira, 2004; Graf et al., 1994). Malatya HMS shows strong positive Eu anomalies (Eu/Eu* = 0.99-1.03). This feature is similar to the shale Eu anomalies (Figs. 6a, b and c) and quite different from the non-distinguishable Eu positive anomalies of Neoproterozoic iron formations (Klein & Ladeira, 2004). Positive Eu anomalies have been attributed to hydrothermal solutions or a detrital feldspar contribution (Campbell et al., 1988; Michard & Albarede, 1986). In the case studied a feldspar contribution is more likely.

La enrichments (La/La* = 0.71-1.15) are not as high as La enrichments of BIFs (La/La* = 5.18, Basta et al., 2011; Roy & Venkatesh, 2009). The Ce anomalies are accepted as an indicator of the oxidation state of the sea water (Elderfield & Greaves, 1982; De Baar et al., 1985). The Ce anomalies (Ce/Ce* = 0.003-0.06) of HMS are very low positive indicating low oxidation state of the sea water during deposition.

6. CONCLUSIONS

The HMS tectonic slice outcrops in a very limited area and without any data of underlying and

overlying formations. Therefore the conclusions are limited to the findings on the HMS itself.

The mineral assemblage and textures of the HMS indicate that the rock was metamorphosed under amphibolite facies conditions and original material was clayey detritus. High Al, Ti and alkaline elements Mg, Na and K denote detrital material had continental origin and magmatic components. The features of the HMS are quite different from the Malatya Metamorphics, which

were metamorphosed under sub-greenschist facies conditions and meta-carbonates are dominant.

Therefore, it is reasonable to relate the HMS tectonic slice to the Pütürge Massif, which is composed of high grade metamorphic rocks: gneiss, augen gneiss, amphibolite, mica schist and marble. The mineral assemblage, hematite-quartz mica kyanite pyroxene garnet, of the HMS is quite different from the mineral assemblages of the BIFs and IFs what usually have a simple mineral assemblage

Table 3. REE contents of the HMS and well-known BIFs of the world. The REE contents originating from detritus and autochthonous materials are not discriminated.

Ppm	QF ¹		QF ¹ Itabirite	QF ² Itabirite	Superior ³ BIF	Algoma ⁴ BIF	This Study		
	Hematite	Itabirite					MYS1	MYS2	MYS3
La	6.51	3.75	1.40	0.22	7.00	1.37	68.50	82.40	71.40
Ce	13.96	5.15	2.32	0.54	12.71	2.73	149.9	171.10	157.30
Pr	1.45	0.90	1.59	0.20	5.49	1.46	16.94	19.76	17.88
Nd	5.45	4.48	0.32	0.06	1.47	3.23	66.40	76.7	68.90
Sm	1.22	0.43	0.43	0.08	1.13	3.05	12.85	13.69	13.50
Eu	0.34	0.37	0.54	0.14	1.51	0.30	4.14	4.05	4.24
Gd	1.04	0.86	0.30	0.09	0.85	0.22	12.18	12.93	12.83
Tb	0.17	0.14	0.35	0.08	0.85	0.23	1.84	2.05	1.87
Ho	0.25	0.16	0.12	ND	0.26	0.07	1.88	2.04	1.87
Er	0.76	0.44	0.09	ND	0.19	0.06	5.15	5.31	5.03
Tm	0.16	0.09	0.56	1.10	1.16	0.34	0.76	0.78	0.75
Yb	0.48	0.43	0.05	ND	0.11	0.03	4.75	4.77	4.46
Lu	0.13	0.08	0.05	0.02	0.13	0.03	0.70	0.69	0.65
ΣLREE	23.64	15.23	6.05	1.10	27.80	11.84	314.59	363.65	328.98
ΣHREE	3.21	1.68	2.21	0.45	5.04	2.93	40.83	43.00	41.33
ΣREE	26.85	16.91	8.26	1.55	32.85	14.78	355.42	406.65	370.31
Eu/Eu*	1.50	1.60	1.49	1.33	1.45	2.13	1.01	0.99	1.04

¹Spier et al., 2007; ²Glikson et al., 2004; ³Klein & Beukes, 1989; ⁴Kato et al., 1996; N.D: not detected.

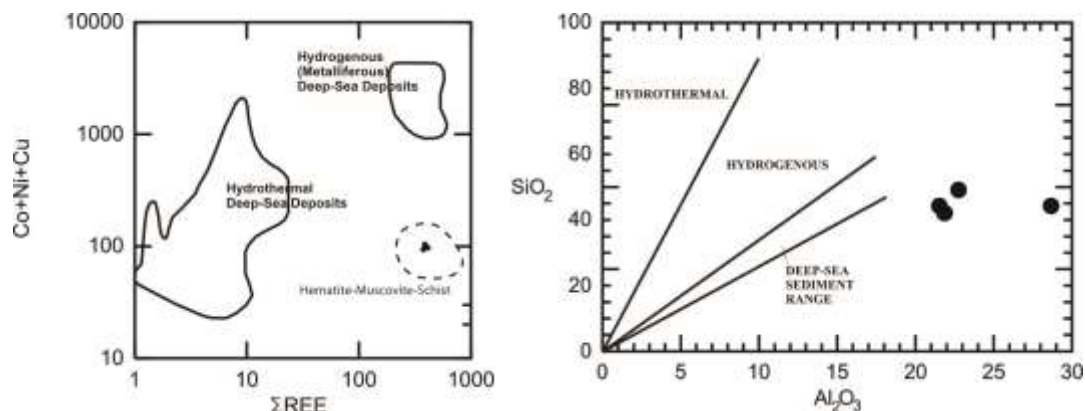


Figure 5. (a) ΣREE Co+Cu+Ni plots of HMS. The HMS plots do not fall in neither hydrothermal nor hydrogenous areas, instead in a distinct area. (b) SiO₂-Al₂O₃ plots of the HMS. Note that the samples fall close to deep sea sediments range.

of quartz and Fe-oxide/carbonate. The Fe mineral is hematite and magnetite is absent this may reflect a well oxygenated environment of formation. However, Ce anomalies show low oxidation state during sedimentation.

The major element contents reflect this difference as relatively higher Al, K, Na, and Ti contents, what may be interpreted as detrital origin. Fe contents of the HMS range from 17.70 to 22.75 % and are close to the lower limit (20 %, Klein, 2005) for BIFs accepted by previous works. SiO₂ contents (41.89-48.76) are within the range of BIFs' SiO₂ contents. Al₂O₃ contents are quite different from those of BIFs and vary between 21.78 and 22.75%. TiO₂ contents (3.32-5.49%) exhibit a similar pattern to Al₂O₃ contents, and they also disagree strongly from TiO₂ contents of BIFs. Al₂O₃ and TiO₂ contents of the HMS are close to the same contents of the upper shale of the iron ore deposits of the Singhbhum-Orissa Belt, India described by Roy & Venkatesh (2009). High Al and Ti contents indicate large amounts of detrital contribution during sedimentation. MgO, Na₂O and K₂O are also higher than those of BIFs and suggest a continental source. High Σ REE and a positive Eu anomaly also support a large detrital contribution. Therefore a hydrothermal source for the HMS and its Fe contents is unlikely.

Trace element contents are also many times higher than those of BIFs and IFs. LREE enrichment is another proof of detrital origin. Positive Eu anomalies could be because of detrital feldspar contribution. Σ REE contents and SiO₂-Al₂O₃ plots indicate deep sea sediments origin. Laminated/banded texture is also accepted as deep sea sedimentation texture (Klein, 2005). The depth should be deeper than 200m which is accepted as the depth limit of wave effect.

Alternating bands/laminae of Fe and Si and major element composition of the HMS are similar features to those of Banded Iron Formations. As the HMS can be related Pütürge Massif the age of it should be Neoproterozoic, the age of the cores of the Anatolian Massifs.

Many Neoproterozoic BIFs are present on the African and Arabian Plates; ANS (Egypt and Saudi Arabia), Menhouhoy (Morocco), Unarab and Wadi Karim (Egypt) and Sawawin (Saudi Arabia) (Basta et al., 2011). They have either volcanic (Algoma Type) or glacial (Rapitan Type) associations (Basta et al., 2011). As the cores of Anatolian massifs are accepted as the northern margins of the Gondwana (Candan et al., 2011), the HMS may be one of the Neoproterozoic BIFs or IFs of the African Plate. High Al contents, LREE enrichment, positive Eu anomalies

and high K, Ca and Na contents all indicate detrital contribution. Evidence of any volcanic and hydrothermal contribution is not present.

From all the above given data it can be concluded that the HMS may be a Neoproterozoic BIF of glacial association (Rapitan Type). However, geochemistry of the HMS is quite different than the composition of the Rapitan Type IFs. The Fe could have concerted in deep sea together with clayey sediments. The iron mineral of the HMS is hematite what forms in highly oxygenated environments and thus apparently does not fit to this model. However, hematite could have not formed in situ instead might have been transported to the depositional place from continental areas or shallow well aerated zones of sea as suspensions of FeO (OH) minute particles.

From the findings of this study, the geological history of the HMS can be summarized as: Hematite Mica Schist of Malatya formed as a detrital sedimentary formation in a basin where the oxidation state was very low due to ice cover, and Fe remained in the solution for long periods and accumulated. Oxidation was caused after the melting of ice cover of oceans and precipitation took place. Such formation models are postulated for Neoproterozoic Iron Formations and Banded Iron Formations what forms stratigraphic sequences of glaciomarine settings and they are the result of anoxic condition resulted from the stagnation in the oceans beneath ice cover (Lyons et al., 2009; Walde & Hagemann, 2007; Klein, 2005; Klein & Ladeira, 2004). The HMS has higher Sm/Lu values (18.35 - 20.76) and lower La/Ce and La/Sm values (0.45-0.48 and 5.29-6.02, respectively) than those of Proterozoic BIFs and these features can be taken as evidences of glaciomarine setting or low sea level (Graf et al., 1994; Kirschvink, 1992).

The HMS of Malatya was probably formed in a sedimentary basin where anoxic conditions were prevailing and iron was abundant in solution because of thick ice cover. Following the ice melt terrestrial sediment input in the basin increased and sediments and iron deposited as alternating layers. As its major element contents are rather similar to the upper shale or lower shale of the North Orissa, India BIF, it is also likely that the HMS is the upper or lower shale of the main BIF deposition. Unfortunately any other formation of the probable sequence of HMS does not surface in the vicinity and it is not possible to model a succession.

Although the Hematite Mica Schist of Malatya is exposed in a very narrow area and does not have any economic potential itself, it provides strong evidence that Banded Iron Formations may exist in the "Massifs" of Anatolia.

ACKNOWLEDGEMENTS

Authors are grateful to Dr. R.M.F Preston UK, for his help to improve the English of the manuscript and critical reading. We also thank to Dr. Z. Ozdemir, Mersin University, for her support in XRF and XRD analysis; I. Altıntaş for his assistance during field work and technicians of Geology Department, Firat University for preparing polished and thin sections and helping sample preparations. Author also thank to Prof. Dr. Marian Lupulescu for her critical review of the manuscript.

REFERENCES

- Anders, B., Reischmann, T., Kostopoulos, D. & Poller, U., 2006. *The oldest rocks of Greece: first evidence for a Precambrian terrain within the Pelagonian Zone*. *Geol. Mag.*, 143(1), 41–58.
- Basta, F.F., Maurice, A.E., Fontbote, L. & Favarger, P.Y., 2011. *Petrology and geochemistry of the banded iron formation (BIF) of Wadi Karim and Um Anab, Eastern Desert, Egypt: Implications for the origin of Neoproterozoic BIF*. *Precambrian Research*, 187, 277–292.
- Bekker, A. & Kaufman, A., 2007. *Oxidative forcing of global climate change: a biogeochemical record across the oldest Paleoproterozoic ice age in North America*. *Earth and Planetary Science Letters*, 258, 486–499.
- Bekker, A., Slack, J.F., Planavsky, N., Krapez, B., Hofmann, A., Konhauser, K.O. & Rouxel, O.J., 2010. *Iron formation: the sedimentary product of a complex interplay among mantle, tectonic, oceanic and biospheric processes*. *Economic Geology*, 105, 467–508.
- Bhattacharya, H.N., Chakraborty, I. & Ghosh, K.K., 2007. *Geochemistry of some banded iron formations of the Archean supra crustals, Jharkhand-Orissa region, India*. *J. Earth Syst. Sci.*, 116(3), 245–259.
- Bozkaya, Ö., Gürsu, S. & Göncüoğlu, M. C., 2006. *Textural and mineralogical evidence for a Cadomiantectonothermal event in the eastern Mediterranean (Sandıklı-Afyon area, western Taurides, Turkey)*. *Gondwana Research*, 10(3–4), 301–315.
- Bozkaya, Ö., Yalçın, H., Başibüyük, Z., Özfirat, O. & Yılmaz, H., 2007. *Origin and evolution of the southeast Anatolian metamorphic complex (Turkey)*. *Geologica Carpathica*, 58(3), 197–210.
- Bozkurt, E., Winchester, J.A., Yigitbas, E. & Ottley, C.J., 2008. *Proterozoic ophiolites and mafic-ultramafic complexes marginal to the Istanbul Block: an exotic terrane of Avalonian affinity in NW Turkey*. *Tectonophysics*, 461(1–4), 240–251.
- Bozkurt, E., Winchester, A.J., Mittwede, S. & Ottley, C., 2006. *Geochemistry and tectonic implications of leucogranites and tourmalines of the southern Menderes Massif, southwest Turkey*. *Geodin. Acta*, 19/5, 363–390.
- Bozkurt, E., Park, R.G. & Winchester, J.A., 1993. *Evidence against the core/cover interpretation of the southern sector of the Menderes Massif, West Turkey*. *Terra Nova*, 5, 445–451.
- Campbell, A. C., Palmer, M. R., Klinkhammer, G. P., Bowers, T. S., Edmond, J. M., Lawrence, J. R., Casey, J. F., Thompson, G., Humphris, S., Rona, P. & Karson, J. A., 1988. *Chemistry of hot springs on the Mid-Atlantic Ridge*. *Nature*, 335, 514–519.
- Candan, O., Koralay, O.E., Akal, C., Kaya, O., Oberhänsli, R., Dora, O.Ö., Konak, N. & Chene, F., 2011. *Supra-Pan-African unconformity between core and cover series of the Menderes Massif/Turkey and its geological implications*. *Precambrian Research*, 184, 1–23.
- De Baar, H. J.W., Bacon, M. P. & Brewer, P. G., 1985. *Rare earth elements in the Pacific and Atlantic Oceans*. *Geochim.Cosmochim.Acta*, 49, 1943–1959.
- Elderfield, H. & Greaves, M. J., 1982. *The rare earth elements in seawater*. *Nature*, 296, 214–219.
- Eyles, N. & Januszczak, N., 2004. *Zipper-rift: a tectonic model for Neoproterozoic glaciations during the breakup of Rodinia after 750 Ma*. *Earth-Science Reviews*, 65, 1–73.
- Figueiredo - Silva, R., Lobato, L.M., Rosière, C.A., Zucchetti, M., Hagemann, S.G., Baars, F.J., Morais, R. & Andrade, I., 2008. *Hydrothermal origin for the jaspilite-hosted, giant Serra Norte iron ore deposits in the Carajás mineral province, Pará State, Brazil*. *Reviews in Economic Geology*, 15, 255–290.
- Freitas, B.T, Warren, L.V., Boggiani, P.C., Almeida, R.P. & Piacentini, T., 2011. *Tectono-sedimentary evolution of the Neoproterozoic BIF-bearing Jacadigo Group, SW-Brazil*. *Sedimentary Geology*, 238, 48–70.
- Gessner, K., Collins, A., Ring, U. & Gungor, T., 2004. *Structural and thermal history of a poly-orogenic basement: U/Pb geochronology of granitoid rocks in southern Menderes Masif Western Turkey*. *J. Geol. Soc. Lond.*, 161, 93–101.
- Glikson, A.Y., Allen, C. & Vickers, J., 2004. *Multiple 3.47-Ga-old asteroid impact fallout units, Pilbara Craton, Western Australia*. *Earth Planet. Sci. Lett.*, 7040, 1–14.
- Graf Jr, J.L., O'Connor, E.A. & Van Leewen, P., 1994. *Rare earth element evidence of origin and depositional environment of Late Proterozoic ironstone beds and manganese oxide deposits, SW Brazil and SE Bolivia*. *Journal of South American Earth Sciences*, 7(2), 101–233.
- Gutzmer, J., Chisonga, B.C., & Beukes N.J., 2008. *The Geochemistry of Banded Iron Formation-Hosted High-Grade Hematite-Martite Iron Ores*. *Economic Geology*, 15, 157–183.
- Holland, H.D., 1984. *The Chemical Evolution of the Atmosphere and Oceans*. Princeton University Press, Princeton, p. 582.

- Ilyin, A.V.**, 2009. *Neoproterozoic banded iron formations*. *Lithology and Mineral Resources*, 44, 78–86.
- Kato, Y., Kawakami, T., Kano, T., Kunugiza, K. & Swamy, N.S.**, 1996. *Rare-earth element geochemistry of banded iron formations and associated amphibolite from the Sargur belts, South India*. *J. Southeast Asian Earth Sci.*, 14, 161–164.
- Kirschvink, J.L.**, 1992. *Late Proterozoic low-latitude global glaciation: the snowball Earth*. In: **Schopf, J.W., Klein, C.** (Eds.), *The Proterozoic Biosphere: A Multidisciplinary Study*. Cambridge University Press, 51–52.
- Klein C. & Beukes N.J.**, 1989, *Geochemistry and sedimentology of a facies transition from limestone to iron-formation deposition in the Early Proterozoic Transvaal Supergroup, South Africa*. *Economic Geology*, 84, 1733–1774.
- Klein, C. & Beukes, N. J.**, 1992. *Time distribution, stratigraphy, and sedimentologic setting, and geochemistry of Precambrian iron-formations*. In Schopf: **J. W. and Klein, C.** (Eds.), *The Proterozoic Biosphere: A Multidisciplinary Study*. Cambridge, University of Cambridge, 139–146.
- Klein, C. & Beukes, N.J.**, 1993. *Sedimentology and geochemistry of glaciogenic Late Proterozoic Rapitan iron-formation in Canada*. *Economic Geology*, 88, 542–565.
- Klein, C. & Ladeira, E.A.**, 2002. *Petrography and geochemistry of the least altered banded iron-formation of the Archean Carajás Formation, northern Brazil*. *Economic Geology*, 97, 643–651.
- Klein, C. & Ladeira, E.A.**, 2004. *Geochemistry and mineralogy of Neoproterozoic banded iron formations and some selected, siliceous manganese formations from the Urucum district, Mato Grosso do Sul, Brazil*. *Economic Geology*, 99, 1233–1244.
- Klein, C.**, 2005. *Some Precambrian banded iron-formations (BIFs) from around the world: their age, geologic setting, mineralogy, metamorphism, geochemistry, and origin*. *Am. Miner.*, 90, 1473–1499.
- Kump, L.R. & Seyfried Jr, W.E.**, 2005. *Hydrothermal Fe fluxes during the Precambrian: effect of low oceanic sulfate concentrations and low hydrostatic pressure on the composition of black smokers*. *Earth and Planetary Science Letters*, 235, 654–662.
- Küpel, Ş., Ayhan, A., Döyen, A. & Arık, F.**, 2007. *C, O, S and Sr isotope studies on the genesis of Fe-carbonate and barite mineralizations in the Attepe iron district (Adana, Southern Turkey)*. *Chemie der Erde - Geochemistry*, 67/4, 313–322.
- Lyons, T.W., Anbar, A.D., Severmann, S., Scott, C. & Gill, B.C.**, 2009. *Tracking euxinia in the ancient ocean: a multiproxy perspective and Proterozoic case study*. *Annual Review of Earth and Planetary Sciences*, 37, 507–534.
- McClung, C.R.**, 2006. *Basin analysis of the Mesoproterozoic Bushmanland Group of the Namaqua metamorphic province, South Africa*. Unpublished Ph.D. thesis, Auckland Park, University of Johannesburg, 307 p.
- Michard, A. & Albaredé, F.**, 1986. *The REE content of some hydrothermal fluids*. *Chem. Geol.*, 55, 51–60.
- Morris, R.C.**, 1993. *Genetic modelling for banded iron-formation of Hamersley Group, Pilbara Craton, Western Australia*. *Precambrian Research*, 60, 243–286.
- MTA**, 2002. *Geological Map of Turkey, scale 1:500 000, Sivas Sheet*. MTA Ankara.
- Oberhansli, R., Candan, O., Dora, O.O. & Durr, S.**, 1997. *Eclogites within the Menderes Massif, western Turkey*. *Lithos*, 41, 135–150.
- Oberhansli, R., Candan, O. & Wilke, F.**, 2010. *Geochronological Evidence of Pan-African Eclogites from the Central Menderes Massif, Turkey*. *Turkish J. Earth Sci.*, 19, 431–447.
- Özgül, N.**, 1976. *Basic geological features of Taurids*. *Türkiye Jeol. Kur. Bül.*, 19, 65–78 (in Turkish with English abstract).
- Pecoits, E., Gingras, M., Aubet, N. & Konhauser, K.**, 2008. *Ediacaran in Uruguay: palaeoclimatic and palaeobiological implications*. *Sedimentology*, 55, 689–719.
- Pelletier, E., Cheilletz, A., Gasquet, D., Mouttaqi, A., Annich, M. & El Hakour, A.**, 2006. *Discovery of Neoproterozoic banded iron formation (BIF) in Morocco*. *Geophysical Research, Abstracts* 8, European Geosciences Union. 303, 795–797.
- Roy, S. & Vanketash, A. S.**, 2009. *Mineralogy and geochemistry of banded iron formation and iron ores from eastern India with implications on their genesis*. *J. Earth Syst. Sci.*, 118(6), 619–641.
- Scott, C., Lyons, T.W., Bekker, A., Shen, Y., Poulton, S.W., Chu, X. & Anbar, A. D.**, 2008. *Tracing the stepwise oxygenation of the Proterozoic ocean*. *Nature*, 452, 456–459.
- Spier, C.A., de Oliveira, S.M.B., Sial, A.N. & Rios, F.J.**, 2007. *Geochemistry and genesis of the banded iron formations of the Caue Formation, Quadrilátero Ferrífero, Minas Gerais, Brazil*. *Precambrian Research*, 152, 170–206.
- Sunal G., Satir M., Natal'in B. A. & Toraman, E.**, 2008. *Paleotectonic position of the Strandja massif and surrounding continental blocks based on zircon Pb-Pb age studies*. *International Geology Review*, 519–545.
- Ustaömer, P.A., Mundil, R. & Renne, P.**, 2005. *U/Pb and Pb/Pb zircon ages for arc-related intrusions of the Bolu Massif (W Pontides, NW Turkey): evidence for Late Precambrian (Cadomian) age*. *Terra Nova*, 17, 215–223.
- Walde, D.H.G. & Hagemann, S.G.E.**, 2007. *The Neoproterozoic Urucum/Mutún Fe and Mn deposits in W-Brazil/SE-Bolivia: assessment of ore deposit models*. *Zentralblatt für Geologische Geowissenschaften*, 158 (1), 45–55.
- Yazgan, E.**, 1984. *Geodynamic evolution of Eastern*

Taurus Region. Geology of Taurus Belt, Int. Symposium Proceedings, 199-208.
Yılmaz, H., 1991. *Geology of Sürgü area (Doğanşehir,*

Malatya), in the Eastern Taurus. Cumhuriyet Univ. Dergisi, 16/1, 95-106 (in Turkish with English abstract).

Received at: 22. 02. 2013
Revised at: 13. 06. 2013
Accepted for publication at: 18. 06. 2013
Published online at: 24. 06. 2013